# Energetic Particles in the Heliosphere

Horst Fichtner

Institut für Theoretische Physik IV, Ruhr-Universität Bochum, 44780 Bochum, Germany
Presenter: Horst Fichtner (hf@tp4.rub.de)

The contributions to the sessions SH 1.5, SH 2.6 and SH 3.1-6 of the 29th International Cosmic Ray Conference are summarized. The structure of this summary is guided by the physics covered in the about 125 actually presented contributions and, while covering all material, puts emphasis on new observations, newly defined problems and new ideas.

1. Introduction

In this report the presentations during the sessions SH 1.5, SH 2.6 and SH 3.1-6 of the 29th ICRC are divided into six groups, five of which are defined by the physics covered, namely *Solar Activity and Ground Level Enhancements*, *Structures in the Interplanetary Medium*, *Space Weather*, *Cosmic Ray Transport and Modulation*, and *The Outer Heliosphere*. The sixth group contains *New Experiments and Instrumentation*. The report does not contain those submitted papers that were not been presented at the meeting. The majority of studies is, naturally, concerned with a continuation or extension of earlier measurements, the checking of the validity or usefulness of various correlations, and the comparison of model results with data. While all these aspects are covered, the report concentrates on the few 'highlights' of the sessions in order to make clear what is new, i.e., where progress was made and where new problems emerged.
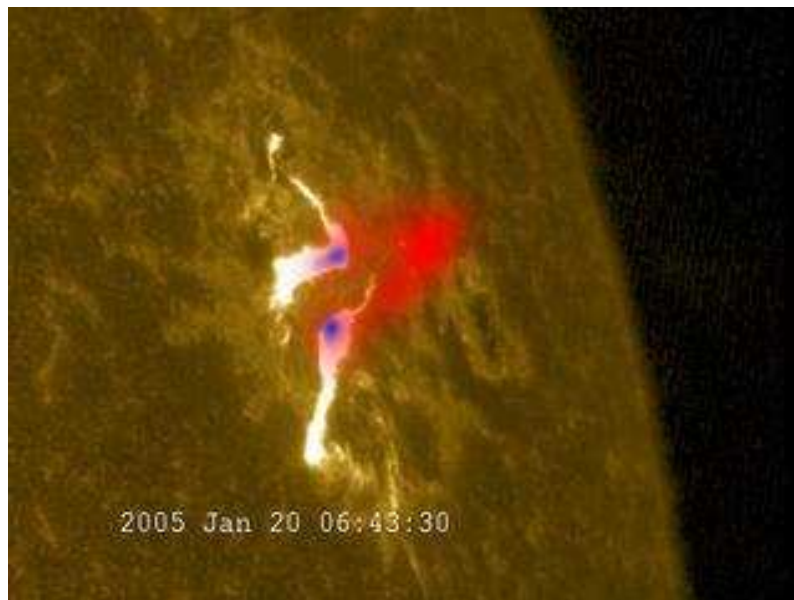
Figure 1. A UV images from the TRACE spacecraft with RHESSI spacecraft images of gamma-rays (blue) and X-rays (red) overlayed, taken from http://svs.gsfc.nasa.gov/vis/a000000/a003100/a003162/. Consult the electronic version of the manuscript for color figures.

## 2. Solar Activity and Ground Level Enhancements

On January 20, 2005, the Sun produced a radiation burst that caused the largest ground level enhancement (GLE) observed on Earth in half a century. The burst was recorded with the TRACE as well as the RHESSI spacecraft (Fig. 1). As a consequence of this burst, over a 6-minute span on January 20, 2005, the neutron rate at the sea level station of McMurdo, Antarctica, increased by a factor of 30 (Bieber et al. [17]). The rate at the high-altitude (2820 m) station of South Pole increased by a factor of even 56. As shown in Fig. 2, other stations observed an increase of only a factor of three or so. Apparently this event was extremely anisotropic.
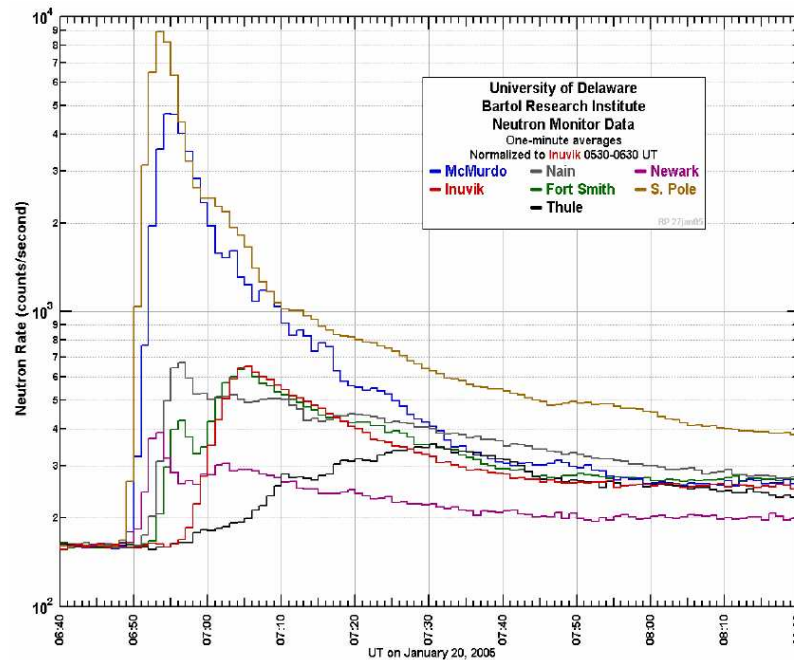
Figure 2. On January 20, 2005 the Sun emitted cosmic rays of sufficient energy and intensity to increase radiation levels on Earth's surface. The GLE was especially intense at South Pole (highest peak) and McMurdo, Antarctica (second highest), where radiation levels increased by factors of 56 and 30, respectively, in a span of six minutes. The McMurdo increase was the largest observed at sea level since 1956 (Bieber et al. [17]).

The significance of this observation is two-fold. First, it is important to note the extremely large fluctuations in magnitude that solar particle events display. This must be taken into account when planning for radiation hazard mitigation in future human missions into deep space (see also the section on space weather below). Second, analyzing this event with modern instrumentation and methods affords an excellent opportunity for studying relativistic solar particle events with unprecedented precision. Such an analysis has been done by Saiz et al. [101] on the basis of the well-established transport equation for solar energetic particles that includes their streaming, (differential) convection, focusing, scattering and deceleration (Ruffolo 1995 [98]). The result of this modelling is shown in Fig. 3.

The data indicate two enhancements in particle flux at Earth, the second of which has a much lower anisotropy. The authors found that the GLE is best modelled by assuming different scattering conditions at the start and
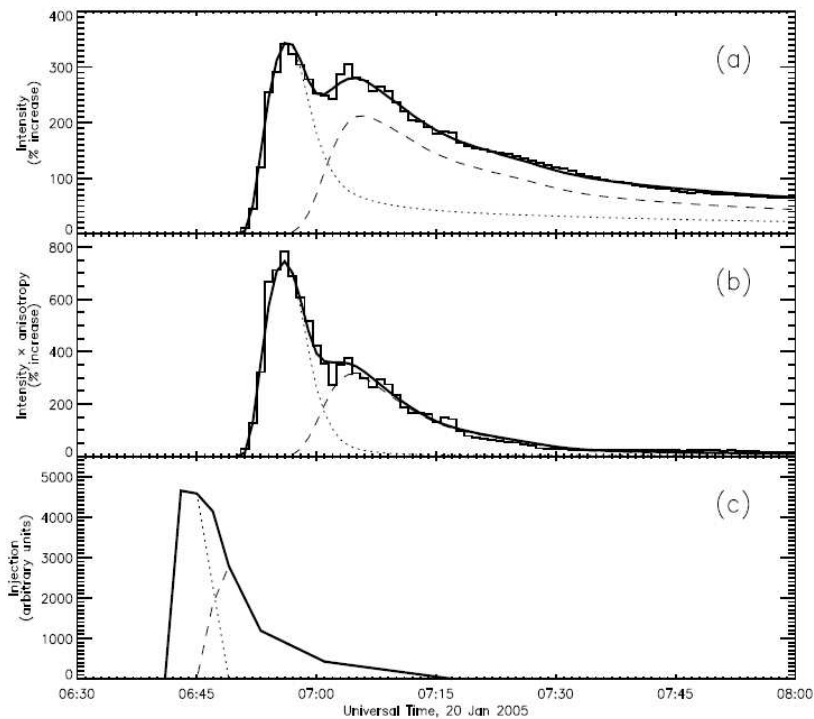
Figure 3. (a) Thin solid line: directionally averaged intensity at polar neutron monitors. Thick line: combination of two solutions to the linear transport equation, one with low scattering conditions (dotted line) and one with higher scattering conditions (dashed line), that best fits the data. (b) Same as (a), but for the weighted anisotropy at polar neutron monitors. (c) Model injection function (solar time) of relativistic solar protons, optimized to fit intensity and weighted anisotropy (Saiz et al. [101]).

later during the event and with a smoothly varying injection time profile. They proposed that the transport conditions changed rapidly during the event due to the high density of solar energetic paticles (SEPs), which generated waves that resonantly scattered the particles injected later in the event (see also Timofeev et al. [120]). These waves are supposedly generated at low wave number in the interplanetary medium even ∼ 1 AU ahead of the shock that is driven by the accompanying coronal mass ejection (CME). These results appear to be consistent with observations of moderate energy SEPs that show the anisotropy of particles streaming away from the Sun to decay faster for larger events than for small ones. As the authors point out, the results indicate that, while one is able to explain the observations satisfactorily with test particle simulations, self-consistent modelling remains desirable.

Miyasaka et al. [81] have derived the proton spectrum for this event (Fig. 4) using the Tibet YBJ Neutron monitor observatory. In addition, the authors mention that no solar neutrons were observed during the event, consistent with the findings reported by Zhu et al. [132], who analysed the same data, and by Moraal et al. [82], who used the SANAE and Tsumeb neutron monitors in South Africa. This result suggests that, unlike for the October 28, 2003, event that was also studied in some detail by Vashenyuk et al. [126], the solar neutron signals, if any, were buried in the main GLE signal. Other papers dealing with the January 20, 2005 event, coming to similar conclusions, were presented by Vashenyuk et al. [127], Belov et al. [10] and Vashenyuk et
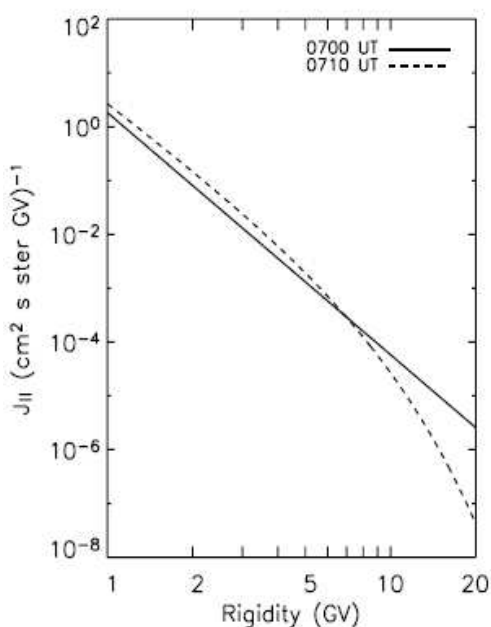
Figure 4. The derived solar proton rigidity spectra at Earth at 07:00 UT (solid line) and 07:10 UT (dashed line) for the January 20, 2005 event (Miyasaka et al. [81]).

al. [128]. Karpov et al. [46], [47] presented a statistical analysis of GLEs during solar cycles 21-23 based on neutron monitor and muon telescope data.

There is an ongoing debate whether the CME-driven shock or the flare is the site of the acceleration of SEPs. Simnett & Roelof [107] argued, based on timing of the various emissions connected with the event, that the protons responsible for the ground level neutron monitor event and those electrons detected by the ACE spacecraft with a very hard spectral index were accelerated in a process or processes directly related to the solar flare (see also Timofeev et al. [120]), and not by the CME, which was probably responsible for delaying the release of the flare electrons. Also Martirosyan & Chilingarian [74] used timing arguments, and even claimed contradictions with common theories of solar particle acceleration. The prevailing view amongst most researchers is, nonetheless, that the CME shock is the acceleration site as, e.g. expressed by Ryan et al. [99].

3.   Structures in the Interplanetary Medium

The January 20, 2005 GLE occured like several other major GLEs during a Forbush decrease, see Fig. 5. A general correlation of CMEs, as a result of which GLEs can occur, with Forbush decreases has been confirmed by Kahler & Simnett [45], who selected all Forbush decreases with a $> 2\%$ decrease observed with the neutron monitor in Oulu, Finland, and checked for their correlation with CMEs. The CME data were provided by the Solar Mass Ejection Imager (SMEI), launched into polar Earth orbit in January 2003. SMEI allows one to search for the white light signatures of interplanetary CMEs and is unique in that it can monitor the progress of CMEs through the inner heliosphere out to distances beyond 1 AU. It can also distinguish those which hit the Earth from those that do not. An excellent correlation of CMEs with Forbush decreases was found.
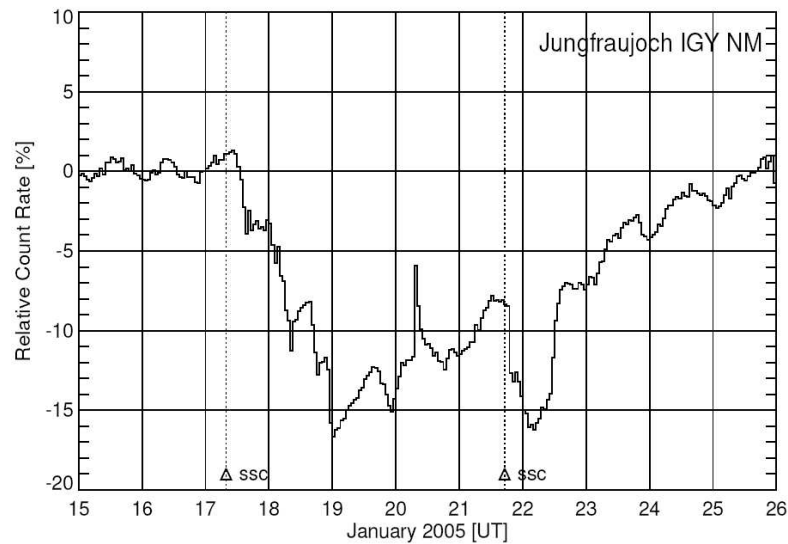
Figure 5. Relative count rate (hourly values) of the IGY neutron monitor at Jungfraujoch for the time interval January 15-25, 2005 Flückiger et al. [37].

A statistical analysis of major solar flares, halo CMEs and Forbush decreases by Shrivastava [106] resulted in the finding that flares in the western solar hemisphere are slightly more likely to be effective in causing Forbush decreases. The local and non-local geometry of interplanetary CMEs was studied by Mulligan et al. [85] with the aid of a non-force-free magnetic flux rope model in conjunction with particle data. They found that changes in the associated Forbush decreases and recovery rates of the cosmic ray intensity depend on non-local, three-dimensional characteristics of an interplanetary CME shock.

The modelling of Forbush decreases themselves has progressed far beyond a qualitative level as was nicely demonstrated by Alania & Wawrzynczak [2] and Alania et al. [3]. These authors presented the idea that the
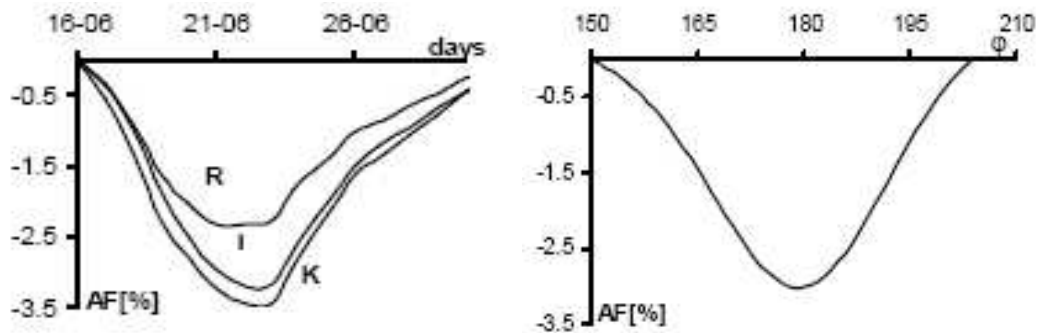

Figure 6. Left: Temporal changes of the cosmic ray intensity for June 16–30, 2003, as observed with the Rome (R), Irkutsk (I), and Kiel (K) neutron monitors. Right: Computed heliolongitudinal variation of the amplitude of the Forbush effect (AF) for 10 GV cosmic rays (Alania & Wawrzynczak [2]; Alania et al. [3]).

power spectral densities of the interplanetary magnetic field, which are significantly higher during the major phase of recurrent (27-day) Forbush effects than before or after, imply a change in the (parallel) cosmic ray diffusion. With a steady-state three-dimensional modulation model they were able to reproduce guantitatively the observed decrease in cosmic ray intensity (Fig. 6) and to show that the cosmic ray rigidity spectrum indeed hardens during a Forbush event.

Belov et al. [11] analysed the use of the (occurrence) frequency and magnitude of Forbush effects as an index of solar activity, in particular of activity bursts, i.e., short time enhancements of the solar sunspot number, the X-ray and the radio fluxes, with the result that it can be used for activity forecasting purposes.

Furthermore, observations of Forbush decreases during October/November 2003 have been reported: Ryan et al. [100] showed that the Milagro telescope, New Mexico, observed a $> 10\%$ Forbush decrease on October 29, 2003, and, thus, that it can be used to investigate SEPs and galactic cosmic ray modulation by measuring count rates due to secondary muons and electromagnetic showers. Measurements with the lead-free Gulmarg Neutron Monitor, Kashmir, confirmed this finding with a 16% decrease in the (hourly integrated) neutron intensity (Shah et al. [102]). Further indirect observations of Forbush decreases were presented by Nonaka et al. [89] and Nonaka et al. [90]. They discuss the use of the GRAPES-3 Air Shower experiment in Ooty, India, for a determination of a cosmic ray anisotropy related to interplanetary shocks and how the observed muon intensity can be related to Forbush decreases.

4. Space Weather
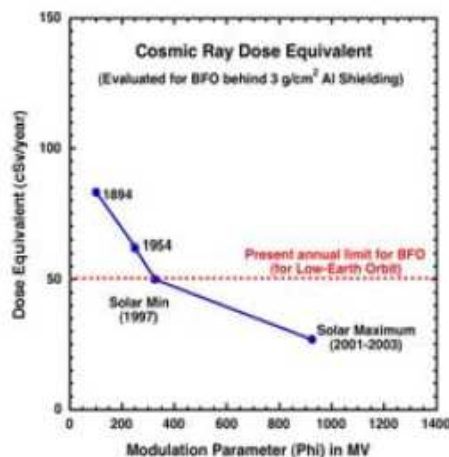
Figure 7. Calculated dose equivalent (in cSv/year) during the ACE solar minimum and maximum periods and during the 1954 and 1984 solar minima (Mewaldt et al. [78]).

A number of presentations were concerned with the effects of energetic particles on the interplanetary radiation conditions as well as on the terrestrial magnetosphere and atmosphere. In particular, radiation risk studies are gaining increasing attention and importance. It was pointed out by Mewaldt et al. [78] that dose limits for astronauts exist only for low-Earth orbits, for which one has 50 cSv/year and 1-4 Sv/career. While there are no limits defined for (deep) space missions such as sending astronauts to the Moon or to Mars, at least radiation dose equivalents for such missions have been computed but remain uncertain to 50% or more. Very interesting

is the notion that not only the 11-year cycle of solar activity is important but that extreme radiation conditions can occur as is evidenced by the January 20, 2005 event. Also, the authors estimated the radiation levels of 50 to 100 years ago to be significantly higher than at present, see Fig. 7. The estimated radiation levels during these earlier periods are up to ~1.7 times greater than during recent solar minima. Depending on the interstellar spectrum this value could be as high as 2. Consequently, for the analysis of a worst-case scenario it is important to measure the interstellar spectrum, which could be measured by the two Voyager spacecraft during their remaining life-time of about 15 years (see section 6).

In view of these radiation risks, work on the protection of astronauts has to continue. Contributions to this effort are the studies of the sensitivity of the total dose-equivalent to fragmentation cross-sections in different energy ranges at the International Space Station (ISS) by Lin & Adams [73] and of the radiation and magnetic environment (Altamura et al. [5]) as well as of the cosmic ray intensity on board the ISS (Casolino et al. [23]). Tripathi [123] pointed out that, while current technology is adequate for single lunar missions for casual astronauts, revolutionary shielding materials are needed for career and deep space astronauts.

Also of interest is the prediction of the energetic particle fluxes for given events. While the rise time of only six minutes for the January 20, 2005 event, makes a prediction almost impossible, it appears that for more 'normal' events particle fluxes can be forecasted a few days ahead (Dorman et al. [31]).

The effects of solar activity on the terrestrial magnetosphere and atmosphere were the subjects of studies by Kumar et al. [63] and Kumar et al. [64] correlating geomagnetic storms with polar coronal holes and sunspot number, respectively, and by Yanke et al. [130] and Chilingarian et al. [26] analysing geomagnetic cut-off rigidity changes during, e.g., the January 20, 2005 event. A correlation of solar activity with the global sea surface temperature was claimed by Shah & Mufti [103].

Geomagnetic effects of galactic cosmic rays were also investigated by Belov et al. [12], who looked into cosmic ray variations due to changes in the magnetosphere during the two severe geomagnetic storms in November 2003 and 2004. The first of these events was analysed in the same context by Zazyan & Chilingarian [131] on the basis of data from the Aragats Space Environmental Center, Armenia.

Also studied were tmospheric effects of cosmic rays, such as their potential relation to the total north-atlantic cyclonal activity (Kavlakov [48]), the greenhouse effect (Perov [92], their relation to thunderstorms (Khaerdinov & Lidvansky [49], [50], see also Khaerdinov et al. [51]; Sharma et al. [105]), and the γ-ray production (Cecchini et al. [24]), were studied as well.

The debate on whether the terrestrial climate is predominantly subject to solar (irradiance) forcing or to cosmic ray forcing was not directly addressed in any of the presentations. Rather, Timofeev et al. [121] have proposed the very speculative idea that gravitational waves from the center of the Galaxy might cause atmospheric pressure pulsations.

5. Cosmic Ray Transport and Modulation

5.1 Anisotropies

As at many previous ICRCs the anisotropy of cosmic rays was subject of numerous presentations. In a very interesting paper Kojima et al. [53] follow up on the relation of the observed sidereal 'daily variation' caused by an anisotropy due to the structure of the heliosphere. Disovered in 1998 in muon data (see Fig. 8, left), it has been speculated that this anisotropy of about $\pm(0.07 - 0.08)\%$ with a maximum at $\sim 10^3$ GeV is connected to heliospheric structure (nose/tail, see Fig. 8, right), although it is quite unclear what heliospheric process could have a signature at such high energies.
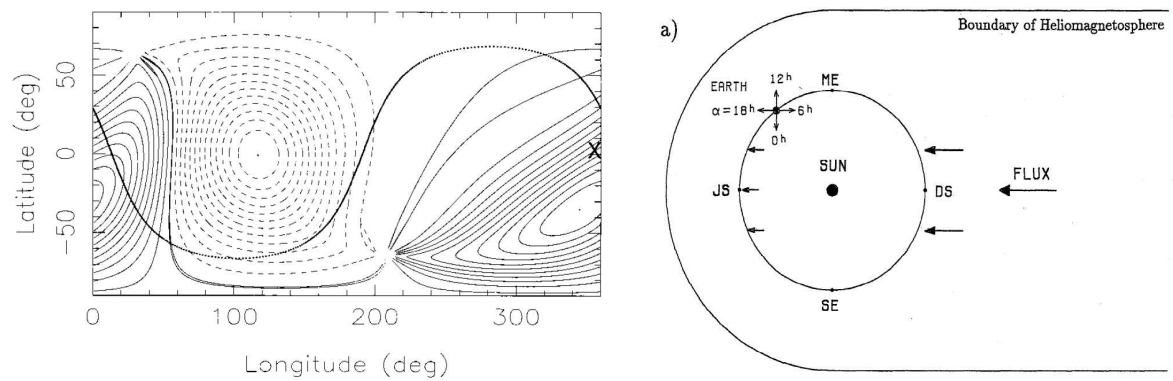
Figure 8. Left: positive (solid lines) and negative (dashed lines) anisotropy in heliospheric coordinates; the cross indicates the downwind direction, and the bold dotted line the galactic equator (Hall et al. 1999 [39]). Right: Annual modulation on the Earth's orbit of the excess fluxes from the heliospheric tail and the associated diurnal harmonic vectors, according to Nagashima et al. (1998, [86]).

Studying γ-ray data Amenomori et al. [6] showed that the anisotropy of $\sim$0.1% extends into the multi-TeV region. Thus, a heliotail effect is even more unlikely than before.

Other studies concentrated on the diurnal variation of cosmic ray intensity (Alania et al. [4]; Amenomori et al. [7]; Braun et al. [19]; Kozyarivsky et al. [56]; Kumar et al. [65], [66], [67]; Moraal et al. [83]; Pandey et al. [91]; Richhariya et al. [97]; Tiwari & Agrawal [122]), on the measurement of the true anisotropy (Kozyarivsky et al. [57]), on the influence of solar wind disturbances on anisotropy (Petukhov et al. [93]), and on the north-south asymmetry (Krymsky et al. [60], [61]).
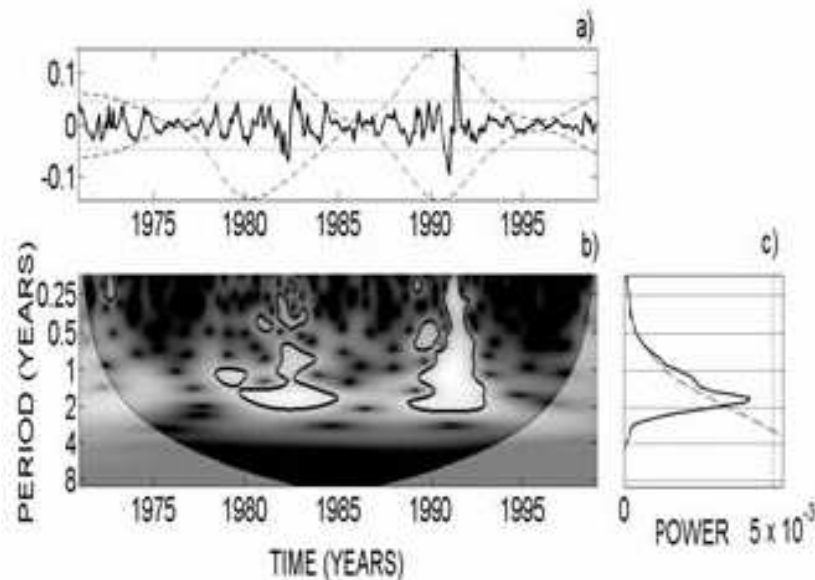
Figure 9. (a) High frequency series of cosmic ray intensity at the Oulu neutron monitor, (b) wavelet and (c) global power spectral density (Valdez-Galicia et al. [125]).

An entirely different anisotropy was discussed by Potgieter et al. [96], namely the inner-heliospheric anisotropy of energetic electrons of Jovian origin, see also Heber et al. [42]. The overall Jovian electron population was modelled with a 3D time-dependent modulation code by Lange et al. [68].

The variation of Sun's shadow during the solar cycle has been looked at with the Tibet Air Shower Array (Amenomori et al. [8]).

5.2   Time variations

Being a traditional topic at ICRCs as well, various time variations of cosmic ray intensity have been studied. In addition to the short-term variations discussed above in the context of Forbush decreases Valdes-Galicia et al. [125] applied the wavelet analysis technique to cosmic ray intensity and solar magnetic flux data estimated in the period 1971-1998. Searching for mid-term variations of 1–2 years they found that the 1.3 and 1.7 year periods, which are discussed in the context of the solar tachocline (i.e. the layer between rigid and differential rotation) and are seen in various solar and interplanetary data, is clearly present also in the cosmic ray data as well (Fig. 9).

Furthermore, the authors found the amplitudes of the corresponding intensity variations to exhibit a dependence on the 11- and 22-year cycle. This dependence and the absence of other mid-term variations suggests that one can rule out the existence of more basic periods than the 11- and 22-year cycle.

The wavelet technique has also been used by Storini et al. [116] for a re-anaylsis of the Climax (CLI), the Huancayo/Haleakala (HH), and the Rome (RM) neutron monitor data (Fig. 10). The authors found the basic 11-year cycle, a 22-year period for Climax, and a 26-year period for Rome/Huancayo-Haleakala, as well as indications of a latitudinal distribution of solar activity in time. Further work is needed to check on these interesting findings.

Miyahara et al. [80] addressed the question whether a 22-year cycle is imprinted in cosmogenic isotope data, as should be expected from the drift-dependent transport of cosmic rays in the heliosphere. Indeed they found such a period during the Maunder and the Spoerer Minimum (Fig. 11) ^{14}C tree ring data. If confirmed, this result is of great signficance as it proves that the solar magnetic field kept reversing even during the Grand Minima of solar activity. For these, and longer, time scales it is important to include effects related to the large-scale structure of the heliosphere, which might change in reaction to internal (solar) as well as external (interstellar) variations. Therefore, hybrid models, such as the modulation model presented by Ferreira & Scherer [33] that takes into account the self-consistent dynamics of the heliosphere, are needed.

Many more presentations have dealt with the 11- and 22-year cycle. The cosmic ray data of recent years (1997–2005) as recorded in the inner heliosphere by ACE and in the outer heliosphere by the Voyager spacecraft were presented by Wiedenbeck et al. [129] and McDonald et al. [75], respectively. Cummings & Stone [29] and Leske et al. [72] derived the intensity gradients of anomalous cosmic rays between 1 AU and the Voyager spacecraft for this period. Ferreira et al. [34] and Heber et al. [43] used Ulysses data to follow up on the compound approach to modulation that combines the effects of the global changes in the heliospheric magnetic field magnitude with drifts to establish a realistic time-dependence in the transport coefficients. Belov et al. [13], Gupta et al. [38], Mishra [79], Sharma [104], Singh & Badruddin [108], Singh et al. [109], and Starodubtsev et al. [110] analysed data of several solar cycles to check on solar activity indices, drift effects, and the cosmic ray fluctuation spectrum. More theoretically inclined work on the heliospheric current sheet evolution and the diffusion tensor was reported by Kota & Jokipii [55] and Alania [1], respectively. Solar cycle modulation at rather high energies of 10–20 GeV was discussed by Braun et al. [19] in the context of muon data recorded with a telescope in Germany.
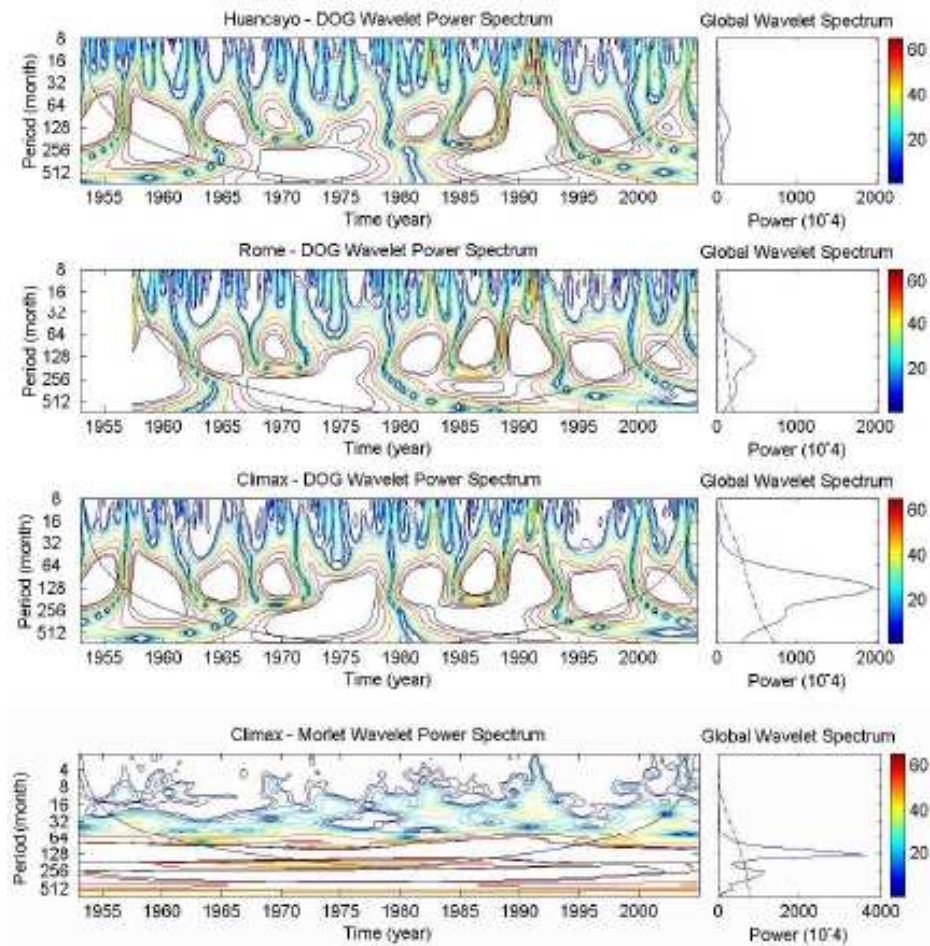
Figure 10. Wavelet power spectrum (left) and global wavelet spectrum (right; with the red noise background, dashed) of CLI, RM and HH data by using Derivative-Of-Gaussian (DOG) (upper panels) and Morlet (lower panel; only for CLI) mother wavelets. Black contours correspond to the 95% confidence level (Storini et al. [116]).

Regarding longer periods Taricco et al. [119] presented an analysis of cosmogenic isotopes (^{44}Ti) in meteorites (Fig. 12). The ^{44}Ti records reveal a variation with a $\sim$100-year period and an amplitude of $\sim$10% as well as a linear trend of decreasing activity ($\sim$27% over 230 years). These records are highly interesting because the cosmogenic isotope archives in meteorites are – unlike those on Earth – unaffected by any atmospheric deposition processes, which could complicate the interpretation of the records tremendously as was pointed out by Nikitin et al. [88] for the example of ^{10}Be. To shed more light on the correlation of the latter with cosmic ray intensity, Moraal et al. [84] reported on a pilot experiment to cut ice from the exposed ice shelf near the South African base, SANAE, in Queen Maud Land, Antarctica, from which data for the five recent decades might be obtained.

Time variations in the records of terrestrial cosmogenic archives due to sporadic events were searched for by
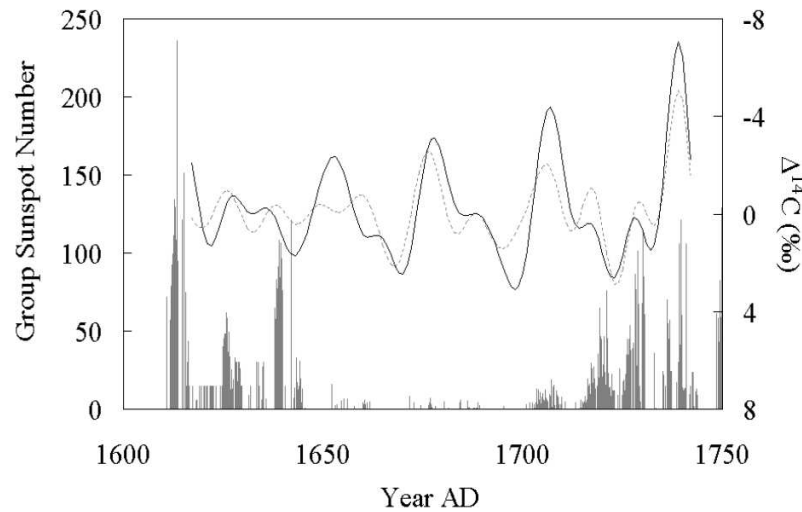
Figure 11. Monthly group sunspot activity and the band-pass filtered carbon-14 records with the bandwidth of 10-35 years. Note that the carbon-14 data are plotted inversely. The time-lag in the carbon cycle has been also taken into account. The solid curve shows the band-pass filtered carbon-14 data obtained by this study, and the dotted curve shows the band-pass filtered carbon-14 data that Stuiver et al. (1998 [117]) obtained earlier (Miyahara et al. [80]).
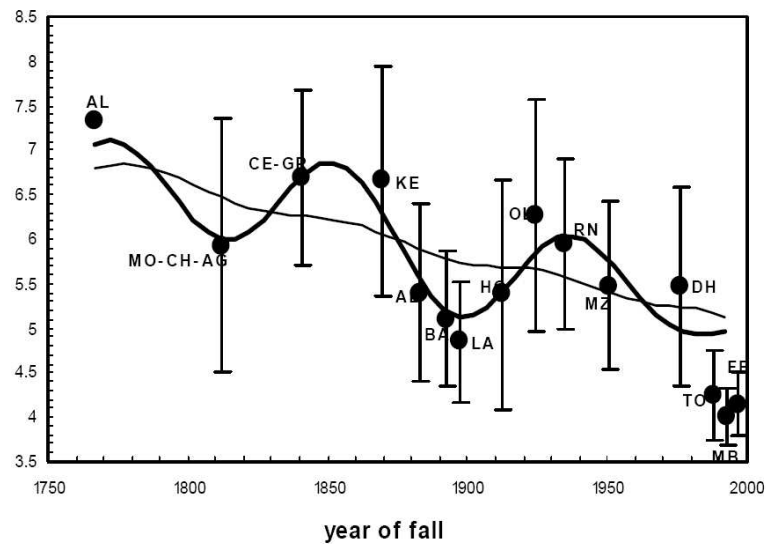
Figure 12. ^{44}Ti activity (dpm/Kg normalized to Fe+Ni concentrations in each chondrite) measured in chondrites: Charsonville (CH), Agen (AG), Cereseto (CE), Grueneberg (GR), Kernouve (KE), Alfianello (AL), Bath (BA), Lancon (LA), Holbrook (HO), Olivenza (OL), Rio Negro (RN), Monze (MZ), Dhajala (DH), Torino (TO), Mbale (MB), Fermo (FE). Superimposed on the data are shown the results of a singular spectrum analysis (curves) (Taricco et al. [119]).
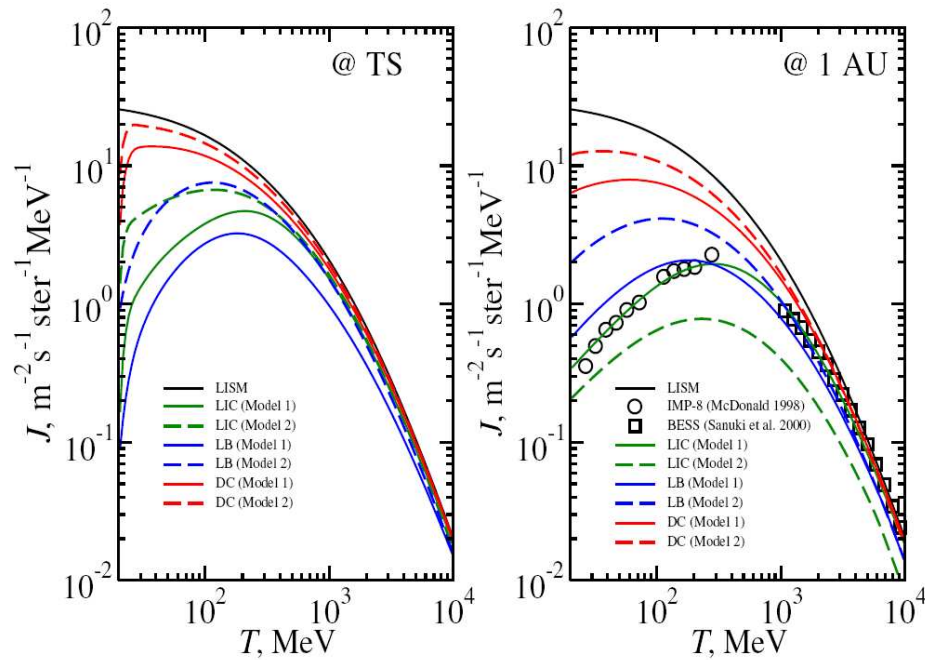
Figure 13. Spectra of galactic protons at 1.1 times the distance to the solar wind termination shock in the apex direction (left) and at 1 AU (right) for the three interstellar environments (Florinski & Zank [35]).

Menjo et al. [77]. They checked tree ring data for signatures of known supernova explosions but could not find any, implying that only rather nearby supernovae could leave an imprint.

For even longer time scales ($10^3 - 10^5$ years) Florinski & Zank [35] modelled the cosmic ray response to heliospheric environment changes and studied the implications for cosmogenic isotope records. They show that a changing interstellar environment can cause the cosmic ray flux at the Earth to be higher or lower than at present (Fig. 13). The resulting estimates of the corresponding ^{10}Be production rates amount to about 80% to 400% of the present rate. The authors remark, however, that these values depend critically on the model of heliospheric turbulence determining the cosmic ray spectra at the Earth.

5.3   Composition

Talavera et al. [118] computed new estimates for the interstellar antiproton spectrum during maximum and minimum solar activity by considering the tertiary component and the antineutron decay especially at energies below ∼1 GeV and improved agreement with observations this way. Potgieter & Langner [95] applied a heliospheric modulation model to model the observed Boron to Carbon ratio (B/C) at Earth, which provides a good measure of the overall secondary to primary ratio of galactic cosmic rays and, thus, makes it an important constraint and test for the validity of numerical models for galactic propagation as well as heliospheric modulation. Finally, Hareyama et al. [40] described measurements of He and Ne isotopes in the terrestrial radiation belts observed with the TSUBASA satellite and argue that the heavy isotopes trapped in the outer radiation belt may have originated from galactic cosmic rays, see also Hareyama et al. [41].

6. The Outer Heliosphere

The participants of the 29th ICRC in Pune, India, could witness a number of highlights being presented at the meeting. One of the highlights was certainly the report on the termination shock crossing of the Voyager 1 spacecraft (Cummings et al. [30]; see also Stone [112] and the highlight paper by Stone). This long-expected event took place on December 16, 2004, as evidenced by various measurements of particle fluxes (for an example see Fig. 14) as well as by the changing strength and characteristics of the heliospheric magnetic field (Fig. 15 and Fig. 16). The termination shock was located at 94 AU at the end of 2005 and, supposedly,
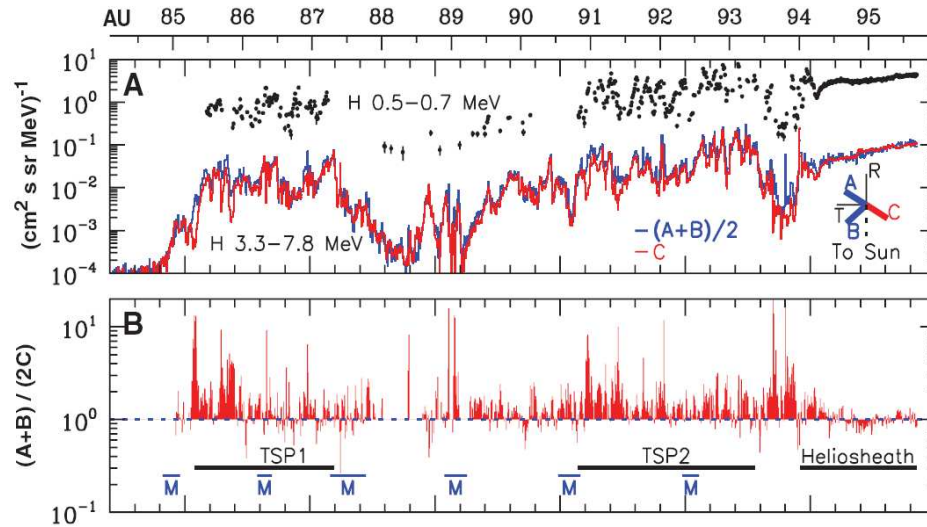
Figure 14. Upper panel: the inset illustrates the telescope viewing directions projected into the R-T plane, where -R is toward the Sun and T is azimuthal. The proton intensity (H) at 3.3 to 7.8 MeV is observed by particle telescopes A plus B that are sensitive to ions streaming outward along the spiral magnetic field in the negative T direction and by telescope C observing in the opposite direction. The intensity of H with 0.5 to 0.7 MeV observed by telescope A is shown for times when the background correction was <60%. Voyager 1 crossed the shock and entered the heliosheath on December 16, 2004. Lower panel: azimuthal streaming index as indicated by the ratio of the average daily intensity in telescopes A and B to that in C. Upstream of the shock, there were two periods of upstream episodes of enhanced intensities (TSP1 and TSP2) during which streaming anisotropy was usually large and mainly in the negative T direction. The streaming anisotropy is much smaller in the heliosheath. Merged interaction regions (labeled M) are indicated as well (Cummings et al. [30], see also Stone et al. (2005 [115])).

was moving inward. The latter deduction follows from the inferred low convection speed of < 40 km/s in the heliosheath and the observation that the intensity of particle fluxes keeps increasing downstream. Both observations could be explained by a inward motion of the shock with a speed of the order of 100 km/s (Jokipii & Kota [44]).

In contrast to the pre-ecounter events TSP1 (in 2002/2003) and TSP2 (in 2004, see Fig. 14) the shock crossing is unequivocally confirmed by the magnetic field measurements in December 2004. While there were, unfortunately, no data recorded on December 16, 2004, a clear compression of a factor of ∼3 can be derived from the data recorded before and after the crossing (Ness et al. [87]), see Fig. 15. Interestingly, no sector boundaries were observed in the heliosheath during the first few months after the shock encounter, giving support to
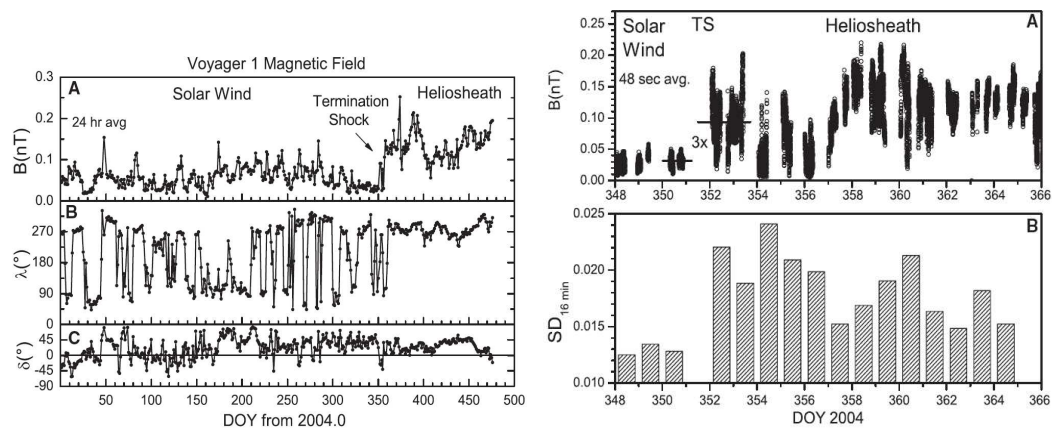
Figure 15. Left: Hourly average magnetic field in heliographic coordinates λ, δ observed by Voyager 1 in 2004/2005. Crossings of sector boundaries/the heliospheric current sheet are evident in 2004, but were not seen after December 16, 2004, i.e. in the heliosheath. Right: 48 second-averaged magnetic field strength B(nT) before and after the termination shock crossing and measurements of daily averaged higher frequency fluctuations up to 0.25 Hz over 16 minute intervals ($SD_{16\,min}$) (Ness et al. [87]; see also Burlaga et al. (2005 [20])).

the idea of a low convection speed of the order of the spacecraft speed. Further evidence for a significantly altered magnetic field in the downstream region comes from its fluctuations, which are much stronger in the heliosheath, see lower right panel of Fig. 15. Finally, also the statistical distribution of field magnitude changed from lognormal (upstream) to gaussian (heliosheath), see right panel of Fig. 16. The left panel of that figure shows a comparison of the predicted and the actually observed field magnitude before and after December 16, 2004.

The recent cosmic ray Helium intensities as observed by both Voyager spacecraft have been modelled with a 2D acceleration/modulation code by Caballero-Lopez et al. [21]. The results are in rather satisfactory agreement with the observations and indicate that cosmic ray transport modelling is, in general, well understood. Nonetheless, problems remain. First, there is the obseration that the anomalous cosmic spectra are still modulated beyond the termination shock, indicating that Voyager has not yet encountered the actual acceleration site of these particles (Cummings et al. [30]; Stone [112]; Stone et al. (2005, [115]). Second, a new energetic particle component – the so-called termination shock particles – being responsible for the pre-encounter events TSP1 and TSP2, as well as another one in the heliosheath (Stone et al. [114]), has been discovered. These particles at energies below about 10 MeV/nucleon exhibit a power law spectrum that often shows no evidence of modulation at the lowest energies, suggesting a nearby source region of termination shock particles, connected to Voyager 1 along the heliospheric magnetic field. As there is modulation at higher energies typical for anomalous cosmic rays, the new component has to be distinguished from the latter. While there exists no generally accepted explanation for the origin of these particles so far (see Florinski et al. [36]), the observational material is increasing. McDonald et al. [76] have shown that the properties of the TSP events are strongly influenced by the passage of interplanetary/heliospheric transients (partially associated with merged interaction regions as indicated in the lower panel of Fig. 14).

It will be very important to analyse the forthcoming analogous data of Voyager 2, when this spacecraft encounters the shock because, unlike its twin, it has well-functioning plasma instruments with which it should be possible to reveal the structure of the shock in detail. Very interestingly, there is evidence that it is approaching
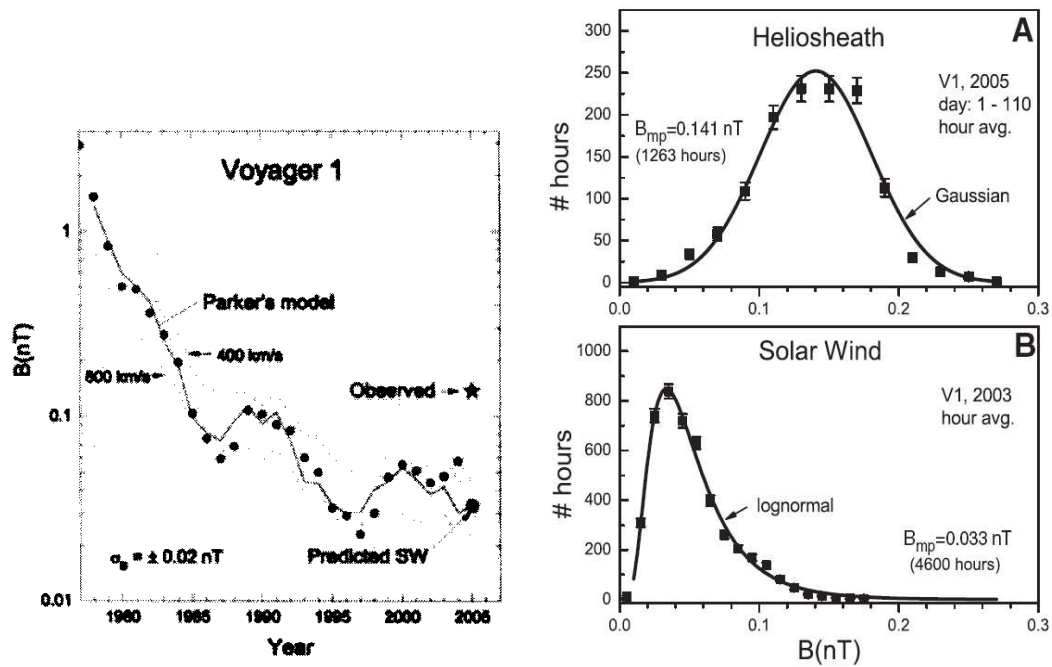
Figure 16. Left: a comparison of the annual averaged magnetic field strength observed by Voyager 2 with the predicted upstream value for December 2004. Right: the statistical distribution of the observed magnetic field strength (upper panel) in the heliosheath and (lower panel) in the upstream solar wind. (Ness et al. [87]; see also Burlaga et al. (2005 [20])).

the shock already. Kiraly [52] compared the > 0.5 MeV/nucleon ion flux recently measured by Voyager 2 with those recorded by Voyager 1 three years ago, see Fig. 18. These data suggest that Voyager 2 might cross the (inward moving?) termination shock within the next two or three years.

In view of these exciting new observations, new and improved approaches to model the structure of the outer heliosphere are needed. Two examples were already presented at the conference. First, there were several studies dealing with the cosmic ray transport in the heliosheath (Caballero-Lopez et al. [22]; Langner & Potgieter [69]; Langner et al. [70]; Potgieter & Langner [94]) with the latter two assuming the heliosheath to be asymmetric as resulting from large-scale modelling of the heliosphere. Second, the injection of pickup ions into the process of diffusive acceleration at the termination shock and their subsequent energization to anomalous cosmic rays has been re-analyzed by Berezhko & Ksenofontov [16], who claim to arrive at essentially different results than published previously by le Roux & Fichtner (1997, [71]).

7. New Experiments and Intrumentation

Several experimental/instrumental developments for new, extended and/or refined measurements have been presented as well. They can be divided as related to ground-based measurements and spacecraft measurements, respectively.
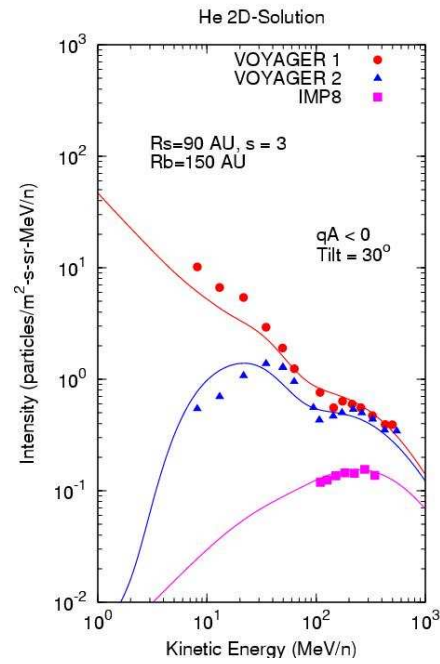
Figure 17. The computed spectra (lines) of cosmic ray Helium compared to the observations by Voyager 1 (downstream, circles), Voyager 2 (upstream, triangles), and IMP 8 (1 AU, squares) (Caballero-Lopez et al. [21]).
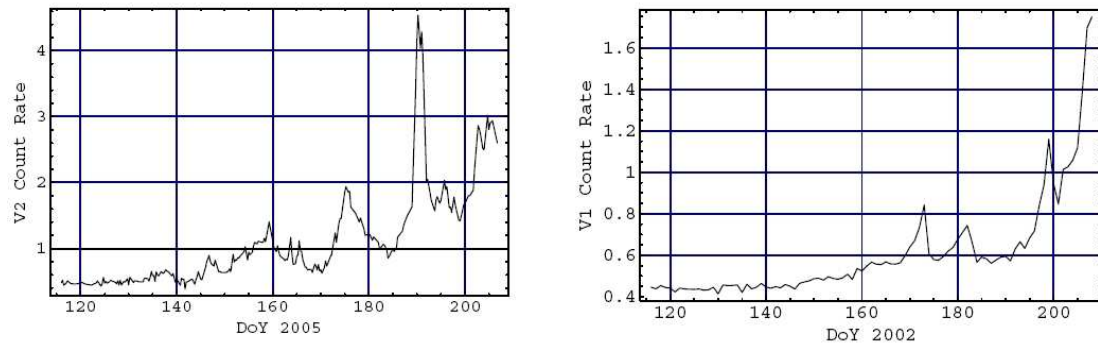
Figure 18. The > 0.5 MeV/nucleon ion flux recently measured by Voyager 2 (left) compared with those recorded by Voyager 1 three years ago (right) (Kiraly [52]).

7.1 Ground-based measurements

A new data base has been presented by Starodubtsev et al. [111]. The authors report on more than a year of operation of the Real-Time Cosmic Ray Distributed (RECORD) database that at present contains 1-min data of cosmic ray intensity collected at five stations Lomnicky Stit, Moscow, Oulu, Tixie Bay and Yakutsk.

Chilingarian et al. [27] have described the Space Weather Observatory at Aragats mountain in Armenia that

allows monitoring of different species of secondary cosmic rays at two high altitude research stations with neutron and muon detectors.

A number of papers concentrated on neutron monitors. Krüger & Moraal [58] analysed the temperature and environmental sensitivity of a recently completed calibration neutron monitor used to calibrate the Sanae neutron monitor. In an accompanying paper Krüger et al. [59] described the performance of a second calibration neutron monitor on three voyages from Seattle to McMurdo, Antarctica, and back. Evenson et al. [32] have presented measurements for neutron counter tubes that are necessary for temperature corrections to the data obtained with the Bartol neutron monitor network, which is part of the Spaceship Earth project. Belov et al. [14] used two independent methods for quantitative estimates of the long-term stability of neutron monitors that operate longer than one solar cycle.

Muon detectors and their characteristics have been discussed by Arakelyan et al. [9], Chernov et al. [25] and Krymsky et al. [62]. Borog et al. [18] presented a new method for continuous monitoring of changes of the vertical temperature profile from the ground level up to the stratosphere by means of muon intensity measurements.

7.2 Spacecraft measurements

Komori et al. [54] described the CALorimetric Electron Telescope (CALET) mission that is proposed to measure galactic electrons and gamma rays on the International Space Station (ISS) for three years after 2010. Electron measurements on ISS were also discussed by Bencardino et al. [15], who reported on the Low Altitude Zone Ionization Observatory (LAZIO) experiment, launched on February 28, 2005, with start of operations aboard ISS in April 2005. LAZIO is a high performance cosmic ray detector able to measure and identify all particles traversing the apparatus, separating nuclei from electrons/positrons in the energy range 10-100 MeV. Finally, Connell et al. [28] presented performance results of the Angle Detecting Inclined Sensor (ADIS) system, which is a highly innovative and uniquely simple detector configuration used to determine the angle of incidence of heavy ions in space instruments.

8.   Summary and Conclusions

What can be considered the most interesting topics of the SH session of the 29th ICRC reported on above? My choice of favourites is as follows:

- *Solar Activity and Ground Level Enhancements:*
  The January 2005 observation of the second largest ground level enhancement ever recorded showed that there can be unusually intense radiation conditions, giving important constraints for radiation risk analyses. The corresponding modelling is quite advanced and able to reproduce the measurements rather satisfactorily, although a need for self-consistent approaches remains outstanding.

- *Structures in the Interplanetary Medium:*
  The cosmic ray transport theory appears to be in good shape in view of the nice modelling results that were obtained for Forbush decreases. The data base for CMEs is rapidly increasing, and the modelling of CMEs is progressing.

- *Space Weather:*
  In view of extreme events and the insight that solar activity is changing also on time scales longer than

11 or 22 years, there is an increasing awareness of radiation risks in space. Procedures for a reliable forecasting of radiation events are under study.

- *Cosmic Ray Transport and Modulation:* Sophisticated (wavelet) analyses of periods in solar activity and cosmic ray intensity variations have been performed. The results are potentially important for the presently ongoing debate regarding solar versus cosmic ray climate forcing. Also interesting in this context is the confirmation that a 22-year period exists in cosmogenic isotope data.

- *The Outer Heliosphere:* The termination shock has been detected by the Voyager 1 spacecraft. Despite a basic agreement with model predictions there were several surprises and new questions have to be answered.

Regarding the last topic it is worth mentioning that the Voyager 2 spacecraft might encounter the termination shock even before the next ICRC. So, come to the 30th ICRC in Mexico to learn more!

Acknowledgements

References

[1] Alania, M.V., Proc. 29th ICRC, Pune, 2, 223 (2005).
 [2] Alania, M.V., et al., Proc. 29th ICRC, Pune, 1, 371 (2005).
 [3] Alania, M.V., et al., Proc. 29th ICRC, Pune, 1, 367 (2005).
 [4] Alania, M.V., et al., Proc. 29th ICRC, Pune, 2, 219 (2005).
 [5] Casolino, M., et al., Proc. 29th ICRC, Pune, 2, 343 (2005).
 [6] Kawata, N. et al., Proc. 29th ICRC, Pune, 2, 77 (2005).
 [7] Amenomori, M., et al., Proc. 29th ICRC, Pune, 2, 49 (2005).
 [8] Amenomori, M., et al., Proc. 29th ICRC, Pune, 2, 207 (2005).
 [9] Arakelyan, K., et al., Proc. 29th ICRC, Pune, 2, 445 (2005).
[10] Belov, A., et al., Proc. 29th ICRC, Pune, 1, 189 (2005).
[11] Belov, A., et al., Proc. 29th ICRC, Pune, 1, 375 (2005).
[12] Belov, A. et al., Proc. 29th ICRC, Pune, 2, 385 (2005).
[13] Belov, A., et al., Proc. 29th ICRC, Pune, 2, 235 (2005).
[14] Belov, A., et al., Proc. 29th ICRC, Pune, 2, 239 (2005).
[15] Bencardino, R., et al., Proc. 29th ICRC, Pune, 2, 449 (2005).
[16] Berezhko, E.G., et al., Proc. 29th ICRC, Pune, 2, 9 (2005).
[17] Bieber, J.W. et al., Proc. 29th ICRC, Pune, 1, 237 (2005).
[18] Borog, V.V., et al., Proc. 29th ICRC, Pune, 2, 381 (2005).
[19] Braun, I., et al., Proc. 29th ICRC, Pune, 2, 135 (2005).

[20] Burlaga, L.F., et al., Science 309, 2027 (2005).
[21] Caballero-Lopez, R.A., et al., Proc. 29th ICRC, Pune, 2, 5 (2005).
[22] Caballero-Lopez, R.A., et al., Proc. 29th ICRC, Pune, 2, 125 (2005).
[23] Casolino, M., et al., Proc. 29th ICRC, Pune, 2, 345 (2005).
[24] Cecchini, S., et al., Proc. 29th ICRC, Pune, 2, 349 (2005).
[25] Chernov, D.V., et al., Proc. 29th ICRC, Pune, 2, 457 (2005).
[26] Chilingarian, A., et al., Proc. 29th ICRC, Pune, 2, 281 (2005).
[27] Chilingarian, A., et al., Proc. 29th ICRC, Pune, 2, 441 (2005).
[28] Connell, J.J., et al., Proc. 29th ICRC, Pune, 2, 481 (2005).
[29] Cummings, A.C., et al., Paper submitted for the 29th ICRC, Pune (2005); ID code usa-cummings-A-abs1-sh32.
[30] Cummings, A.C., et al., Proc. 29th ICRC, Pune, 2, 17 (2005).
[31] Dorman, L.I., et al., Proc. 29th ICRC, Pune, 2, 425 (2005).
[32] Pyle, K. et al., Proc. 29th ICRC, Pune, 2, 485 (2005).
[33] Ferreira, S.E.S., et al, Proc. 29th ICRC, Pune, 2, 253 (2005).
[34] Ferreira, S.E.S., et al., Proc. 29th ICRC, Pune, 2, 251 (2005).
[35] Florinski, V., et al., Proc. 29th ICRC, Pune, 2, 263 (2005).
[36] Florinski, V., et al., Proc. 29th ICRC, Pune, 2, 19 (2005).
[37] Flückiger, E.O., et al., Proc. 29th ICRC, Pune, 1, 225 (2005).
[38] Gupta, M., et al., Proc. 29th ICRC, Pune, 2, 147 (2005).
[39] Hall et al., JGR 104, 6737 (1999).
[40] Hareyama, M., et al., Proc. 29th ICRC, Pune, 2, 121 (2005).
[41] Hareyama, M., et al., Proc. 29th ICRC, Pune, 1, 257 (2005).
[42] Heber, B., et al., Paper submitted for the 29th ICRC, Pune (2005); ID code ger-heber-B-abs1-sh25.
[43] Kunow, H, et al., Paper submitted for the 29th ICRC, Pune (2005); ID code ger-kunow-H-abs1-sh34.
[44] Jokipii, J.R., et al., Proc. 29th ICRC, Pune, 2, 23 (2005).
[45] Kahler, S.W., et al., Proc. 29th ICRC, Pune, 2, 267 (2005).
[46] Karpov, S.N., et al., Proc. 29th ICRC, Pune, 1, 193 (2005).
[47] Karpov, S.N., et al., Proc. 29th ICRC, Pune, 1, 197 (2005).
[48] Kavlakov, S.P., Proc. 29th ICRC, Pune, 2, 295 (2005).
[49] Khaerdinov, N.S., et al., Proc. 29th ICRC, Pune, 2, 389 (2005).
[50] Khaerdinov, N.S., et al., Proc. 29th ICRC, Pune, 2, 393 (2005).
[51] Khaerdinov et al., Electric Field of Thunderclouds and Cosmic Rays: Evidence for Acceleration of Particles (Runaway Electrons), Atmospheric Research (in press)
[52] Kiraly, P., Proc. 29th ICRC, Pune, 1, 339 (2005).
[53] Kojima, H., et al., Proc. 29th ICRC, Pune, 2, 81 (2005).
[54] Komori, Y., et al., Proc. 29th ICRC, Pune, 2, 453 (2005).
[55] Kota, J., et al., Proc. 29th ICRC, Pune, 2, 271 (2005).
[56] Kozyarivsky, V.A., et al., Proc. 29th ICRC, Pune, 2, 93 (2005).
[57] Kozyarivsky, V.A., et al., Proc. 29th ICRC, Pune, Pune, 2, 97 (2005).
[58] Krüger, H., et al., Proc. 29th ICRC, Pune, 2, 477 (2005).
[59] Krüger, H., et al., Proc. 29th ICRC, Pune, 2, 473 (2005).
[60] Krymsky, G.F., et al., Proc. 29th ICRC, Pune, 2, 89 (2005).
[61] Krymsky, G.F., et al., Proc. 29th ICRC, Pune, 2, 231 (2005).
[62] Krymsky et al., Proc. 29th ICRC, Pune, 2, 461 (2005).
[63] Kumar, S., et al., Proc. 29th ICRC, Pune, 2, 307 (2005).
[64] Kumar, S., et al., Proc. 29th ICRC, Pune, 2, 65 (2005).

[65] Kumar, S., et al., Paper submitted for the 29th ICRC, Pune (2005); ID code ind-kumar-S-abs1-sh32.
[66] Kumar, S., et al., Proc. 29th ICRC, Pune, 2, 69 (2005).
[67] Kumar, S., et al., Proc. 29th ICRC, Pune, 2, 155 (2005).
[68] Lange, D., et al., Paper submitted for the 29th ICRC, Pune (2005); ID code ger-lange-D-abs1-sh25.
[69] Langner, U.W., et al., Proc. 29th ICRC, Pune, 2, 119 (2005).
[70] Langner, U.W., et al., Proc. 29th ICRC, Pune, 2, 1 (2005).
[71] le Roux, J.A., Fichtner, H., JGR 102, 17365 (1997)
[72] Leske, R., et al., Paper submitted for the 29th ICRC, Pune (2005); ID code usa-leske-R-abs1-sh32.
[73] Lin, Z.-W., et al.,Proc. 29th ICRC, Pune, 2, 429 (2005).
[74] Martirosyan, H., et al., Proc. 29th ICRC, Pune, 2, 285 (2005).
[75] McDonald, F.B., et al., Paper submitted for the 29th ICRC, Pune (2005); ID code usa-mcdonald-FB-abs3-sh34.
[76] McDonald, F.B., et al., Proc. 29th ICRC, Pune, 2, 35 (2005).
[77] Masuda, K., et al., Proc. 29th ICRC, Pune, 2, 357 (2005).
[78] Mewaldt, R.A., et al., Proc. 29th ICRC, Pune, 2, 433 (2005).
[79] Mishra, M.P., Proc. 29th ICRC, Pune, 2, 159 (2005).
[80] Miyahara, H., et al.,Proc. 29th ICRC, Pune, 2, 199 (2005).
[81] Miyasaka, H., et al., Proc. 29th ICRC, Pune, 1, 241 (2005).
[82] Moraal, H., et al., Proc. 29th ICRC, Pune, 1, 221 (2005).
[83] Moraal, H., et al., Proc. 29th ICRC, Pune, 2, 105 (2005).
[84] Moraal, H., et al., Proc. 29th ICRC, Pune, 2, 405 (2005).
[85] Mulligan, T., et al., Proc. 29th ICRC, Pune, 2, 379 (2005).
[86] Nagashima et al., JGR 103, 17429 (1998).
[87] Ness, N.F., et al., Proc. 29th ICRC, Pune, 2, 39 (2005).
[88] Nikitin, I., et al., Proc. 29th ICRC, Pune, 2, 243 (2005).
[89] Nonaka, T., et al., Proc. 29th ICRC, Pune, 1, 359 (2005).
[90] Nonaka, T., et al., Proc. 29th ICRC, Pune, 1, 363 (2005).
[91] Pandey, G.K., et al., Proc. 29th ICRC, Pune, 2, 167 (2005).
[92] Perov, S.P., Proc. 29th ICRC, Pune, 2, 397 (2005).
[93] Petukhov, I.S., et al., Proc. 29th ICRC, Pune, 2, 101 (2005).
[94] Potgieter, M.S., et al., Proc. 29th ICRC, Pune, 2, 113 (2005).
[95] Potgieter, M.S., et al., Proc. 29th ICRC, Pune, 2, 129 (2005).
[96] Potgieter, M.S., et al., Proc. 29th ICRC, Pune, 2, 109 (2005).
[97] Richharia, M.K., et al., Proc. 29th ICRC, Pune, 2, 171 (2005).
[98] Ruffolo, D., et al., Ap.J. 442, 861 (1995).
[99] Ryan, J.M., Proc. 29th ICRC, Pune, 1, 245 (2005).
[100] Ryan, J.M., Proc. 29th ICRC, Pune, 1, 383 (2005).
[101] Saiz, A., et al., Proc. 29th ICRC, Pune, 1, 229 (2005).
[102] Shah, G.N., et al., Proc. 29th ICRC, Pune, 1, 351 (2005).
[103] Shah, G.N., et al., Proc. 29th ICRC, Pune, 2, 311 (2005).
[104] Sharma, N.K., Proc. 29th ICRC, Pune, 2, 175 (2005).
[105] Sharma, A.S., et al., Paper submitted for the 29th ICRC, Pune (2005); ID code usa-sharma-AS-abs1-sh36.
[106] Shrivastava, P.K., Proc. 29th ICRC, Pune, 1, 355 (2005).
[107] Simnett, G.M., et al., Proc. 29th ICRC, Pune, 1, 233 (2005).
[108] Singh, Y.P., et al., Proc. 29th ICRC, Pune, 2, 73 (2005).
[109] Singh, M., et al., Proc. 29th ICRC, Pune, 2, 139 (2005).

[110] Starodubtsev, S.A., et al., Proc. 29th ICRC, Pune, 2, 247 (2005).
[111] Starodubtsev, S.A., et al., Proc. 29th ICRC, Pune, 2, 465 (2005).
[112] Stone, E.C., Proc. 29th ICRC, Pune, 2, 45 (2005).
[113] Stone, E.C., et al., Proc. 29th ICRC, Pune, 2, 47 (2005).
[114] Stone, E.C., et al., Proc. 29th ICRC, Pune, 2, 43 (2005).
[115] Stone, E.C., et al., Science 309, 2017 (2005).
[116] Storini, M., et al., Proc. 29th ICRC, Pune, 2, 259 (2005).
[117] Stuiver et al., Radiocarbon 40, 1127 (1998).
[118] Talavera, K.C., et al., Proc. 29th ICRC, Pune, 2, 289 (2005).
[119] Taricco, C., et al., Proc. 29th ICRC, Pune, 2, 195 (2005).
[120] Timofeev, V.E., et al., Proc. 29th ICRC, Pune, 1, 205 (2005).
[121] Timofeev, V.E., et al., Proc. 29th ICRC, Pune, 2, 401 (2005).
[122] Tiwari, C.M., et al., Proc. 29th ICRC, Pune, 2, 187 (2005).
[123] Tripathi, R.K., Proc. 29th ICRC, Pune, 2, 437 (2005).
[124] Tripathi, L., et al., Paper submitted for the 29th ICRC, Pune (2005); ID code ind-tripathi-L-abs1-sh34.
[125] Valdes-Galicia, J.F., et al., Proc. 29th ICRC, Pune, 2, 211 (2005).
[126] Vashenyuk, E.V., et al., Proc. 29th ICRC, Pune, 1, 217 (2005).
[127] Vashenyuk, E.V., et al., Proc. 29th ICRC, Pune, 1, 209 (2005).
[128] Vashenyuk, E.V., et al., Proc. 29th ICRC, Pune, 1, 213 (2005).
[129] Wiedenbeck, M.E., et al., Proc. 29th ICRC, Pune, 2, 277 (2005).
[130] Yanke, V.G., et al., Proc. 29th ICRC, Pune, 2, 417 (2005).
[131] Zazyan, M., et al., Paper submitted for the 29th ICRC, Pune (2005); ID code arm-zazyan-M-abs1-sh35.
[132] Zhu, F.R., et al., Proc. 29th ICRC, Pune, 1, 185 (2005).